discrete Bragg peaks. This continuous pattern can therefore be sampled on a finer scale. That sufficient oversampling can lead to a reconstruction was pointed out by Bates[4]. To perform such a reconstruction, Chapman[2] devised a Fienup-type[17] iterative algorithm. Using a strengthened form of this, Miao *et al.*[5] were able not only to perform reconstructions of model data in two and three dimensions, but also to show that the degree of oversampling called for by Bates[4] can be relaxed somewhat for the higher-dimensional cases.

In our experiment we made use of this reconstruction algorithm. The reconstruction from the diffraction pattern of Fig. 2 is shown in Fig. 4. Our phasing algorithm uses knowledge of a finite support which is defined as an enclosing boundary of the specimen. In this reconstruction, we chose a 5.7 μm × 5.7 μm square as the finite support which is larger than the size of the image itself. The initial input to the iterative algorithm was a random phase set and, after about 1,000 iterations, a good reconstruction (Fig. 4) was obtained. The computing time of 1,000 iterations is ~30 min on a 450-MHz Pentium II workstation. Details of the reconstruction procedure are given elsewhere[5,16]. The reconstructed image is consistent with the resolution limit, ~75 nm, set by the angular extent of the CCD detector. The inner portion of the diffraction pattern could also be filled by Fourier processing of a moderate-resolution image of the specimen made with a scanning transmission X-ray microscope[1], whereupon a reconstruction with an almost perfectly clean background was obtained.

We believe that the successful recording and reconstruction of the test pattern reported here is the critical step that will open the way to high-resolution three-dimensional imaging of such structures as small whole cells, or large sub-cellular structures, in cell biology. Extension from two to three dimensions requires that a series of diffraction patterns be recorded as the specimen is rotated around an axis perpendicular to the beam. We have take the first steps in this direction. Model calculations indicate that the iterative algorithm used in this work is able to reconstruct such a data set[5]. To be able to collect the data set from a biological (or other radiation-sensitive) specimen, it would be necessary to keep the specimen near the temperature of liquid nitrogen. Experiments show that specimens at this temperature can withstand a radiation dose up to 10^{10} Gy without observable morphological damage[18,19]. Finally, to improve the resolution without sacrificing specimen size, a CCD detector with more pixels would be needed: such detectors are now commercially available. □

Received 24 March; accepted 8 June 1999.

1. Kirz, J., Jacobsen, C. & Howells, M. Soft X-ray microscopes and their biological applications. *Q. Rev. Biophys.* **28,** 33–130 (1995).
2. Sayre, D. & Chapman, H. N. X-ray microscopy. *Acta Crystallogr. A* **51,** 237–252 (1995).
3. Millane, R. P. Phase retrieval in crystallography and optics. *J. Opt. Soc. Am. A* **7,** 394–411 (1990).
4. Bates, R. H. T. Fourier phase problems are uniquely solvable in more than one dimension. I: underlying theory. *Optik* **61,** 247–262 (1982).
5. Miao, J., Sayre, D. & Chapman, H. N. Phase retrieval from the magnitude of the Fourier transforms of non-periodic objects. *J. Opt. Soc. Am. A* **15,** 1662–1669 (1998).
6. Sayre, D., Kirz, J., Feder, R., Kim, D. M. & Spiller, E. Potential operating region for ultrasoft X-ray microscopy of biological specimens. *Science* **196,** 1339–1340 (1977).
7. Jacobsen, C. & Kirz, J. X-ray microscopy with synchrotron radiation. *Nature Struct. Biol.* **5,** (synchrotron suppl.), 650–653 (1998).
8. Jacobsen, C., Kirz, J. & Williams, S. Resolution in soft X-ray microscopes. *Ultramicroscopy* **47,** 55–79 (1992).
9. Thieme, J., Schmahl, G., Umbach, E. & Rudolph, D. (eds) *X-ray Microscopy and Spectromicroscopy* (Springer, Berlin, 1998).
10. Haddad, W. S. *et al.* Ultra high resolution x-ray tomography. *Science* **266,** 1213–1215 (1994).
11. Lehr, L. 3D x-ray microscopy: tomographic imaging of mineral sheaths of bacteria *Leptothrix ochracea* with the Göttingen x-ray microscope at BESSY. *Optik* **104,** 166–170 (1997).
12. Wang, Y., Jacobsen, C., Maser, J. & Osanna, A. Soft x-ray microscopy with cryo STXM: II. Tomography. *J. Microsc.* (in the press).
13. Howells, M. *et al.* X-ray holograms at improved resolution: a study of zymogen granules. *Science* **238,** 514–517 (1987).
14. Lindaas, S., Howells, M., Jacobsen, C. & Kalinovsky, A. X-ray holographic microscopy by means of photoresist recording and atomic-force microscope readout. *J. Opt. Soc. Am. A* **13,** 1788–1800 (1996).
15. Sayre, D. in *Imaging Processes and Coherence in Physics* (eds Schlenker, M. *et al.*) 229–235 (Springer, Berlin, 1980).
16. Sayre, D., Chapman, H. N. & Miao, J. On the extendibility of X-ray crystallography to noncrystals. *Acta Crystallogr. A* **54,** 233–239 (1998).
17. Fienup, J. R. Phase retrieval algorithm: a comparison. *Appl. Opt.* **21,** 2758–2769 (1982).
18. Schneider, G. & Niemann, B. in *X-ray Microscopy and Spectromicroscopy* (eds Thieme, J., Schmahl, G., Rudolph, D. & Umbach, E.) 25–34 (Springer, Berlin, 1998).
19. Maser, J. *et al.* in *X-ray Microscopy and Spectromicroscopy* (eds Thieme, J., Schmahl, G., Rudolph, D. & Umbach, E.) 35–44 (Springer, Berlin, 1998).
20. Lindaas, S. *et al.* in *X-ray Microscopy and Spectromicroscopy* (eds Thieme, J., Schmahl, G., Rudolph, D. & Umbach, E.) 75–86 (Springer, Berlin, 1998).

Acknowledgements. The decision to try oversampling as a phasing technique was arrived at in a conversation in the late 1980s with G. Bricogne. W. Yun and H. N. Chapman also participated in early parts of this experiment. We thank C. Jacobsen for help and advice, especially with the numerical reconstruction, and we thank him and M. Howells for use of the apparatus[20] in which the exposures were made; we also thank S. Wirick for help with data acquisition. P.C. thanks the Leverhulme Trust Great Britain for supporting the nanofabrication programme at King's College, London. This work was performed at the National Synchrotron Light Source, which is supported by the US Department of Energy. Our work was supported in part by the US Department of Energy.

Correspondence and requests for materials should be addressed to J.M. (e-mail: miao@xray1.physics.sunysb.edu).

Forcing of the cold event of 8,200 years ago by catastrophic drainage of Laurentide lakes

D. C. Barber*, A. Dyke†, C. Hillaire-Marcel‡, A. E. Jennings*, J. T. Andrews*, M. W. Kerwin*, G. Bilodeau‡, R. McNeely†, J. Southon§, M. D. Morehead* & J.-M. Gagnon‖

** Institute for Arctic & Alpine Research, and Department of Geological Sciences, University of Colorado, Boulder, Colorado 80309, USA*
† Geological Survey of Canada, 601 Booth Street, Ottawa K1A 0E8, Canada
‡ Centre de recherche en géochimie isotopique et en géochronologie, Université du Québec à Montreal, Québec H3C 3P8, Canada
§ Center for Accelerator Mass Spectrometry, L-397, Lawrence Livermore National Laboratory, PO Box 808, Livermore, California 94551, USA
‖ Canadian Museum of Nature, PO Box 3443, Station D, Ottawa, Ontario K1P 6P4, Canada

The sensitivity of oceanic thermohaline circulation to freshwater perturbations is a critical issue for understanding abrupt climate change[1]. Abrupt climate fluctuations that occurred during both Holocene and Late Pleistocene times have been linked to changes in ocean circulation[2–6], but their causes remain uncertain. One of the largest such events in the Holocene occurred between 8,400 and 8,000 calendar years ago[2,7,8] (7,650–7,200 ^{14}C years ago), when the temperature dropped by 4–8 °C in central Greenland[2] and 1.5–3 °C at marine[4,7] and terrestrial[7,8] sites around the north-eastern North Atlantic Ocean. The pattern of cooling implies that heat transfer from the ocean to the atmosphere was reduced in the North Atlantic. Here we argue that this cooling event was forced by a massive outflow of fresh water from the Hudson Strait. This conclusion is based on our estimates of the marine ^{14}C reservoir for Hudson Bay which, in combination with other regional data, indicate that the glacial lakes Agassiz and Ojibway[9–11] (originally dammed by a remnant of the Laurentide ice sheet) drained catastrophically ~8,470 calendar years ago; this would have released >10^{14} m^3 of fresh water into the Labrador Sea. This finding supports the hypothesis[2,7,8] that a sudden increase in freshwater flux from the waning Laurentide ice sheet reduced sea surface salinity and altered ocean circulation, thereby initiating the most abrupt and widespread cold event to have occurred in the past 10,000 years.

During the period of deglaciation that preceded the abrupt climate event of 8,400–8,000 calendar years (cal. yr) ago (the '8.2-kyr event'), a remnant Laurentide ice mass occupied Hudson Bay and served as an ice dam for glacial lakes Agassiz and Ojibway[9–12] (Fig. 1). The rapid collapse of ice in Hudson Bay allowed lakes Agassiz and Ojibway, which had previously discharged over spillways southeastwards to the St Lawrence estuary, to drain swiftly northwards through the Hudson Strait to the Labrador Sea[10,13–15].

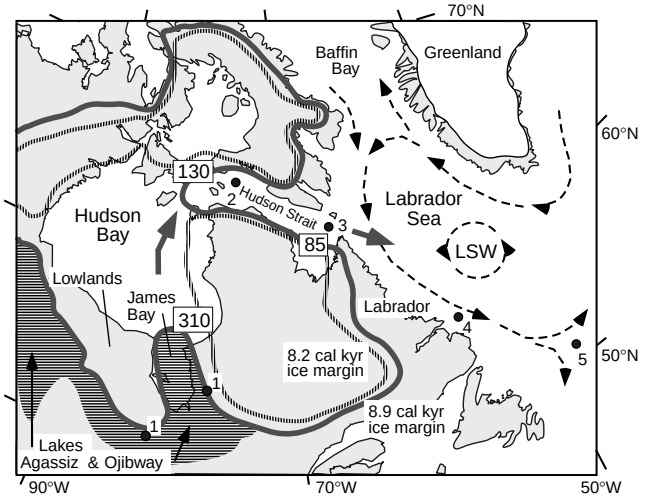

Figure 1 Northeastern Canada and adjacent seas. Former ice-sheet margins[12] are shown for ~8.9 cal. kyr ago (vertical-hatched line) and for ~8.2 cal. kyr ago (thick grey line), before and after disintegration of ice in central Hudson Bay, respectively. Horizontal hatching shows lakes Agassiz and Ojibway[9–12]. Northward drainage through Hudson Bay and Hudson Strait (dark grey arrows) occurred as the Hudson Bay ice mass disintegrated. Arrows with dashed lines show Labrador Sea current patterns and the area of Labrador Sea Intermediate Water (LSW) formation. Numbers in boxes are regional mean ΔR values (years), based on radiocarbon analyses of mollusc shells collected alive before 1955 (ΔR_{local} = ^{14}C age$_{meas.}$–contemporaneous surface ocean ^{14}C age; Table 2). Sites discussed in text and referred to in Table 1 (filled circles) are as follows: site 1, SW and east of James Bay, marine deposits post-dating drainage of glacial lakes Agassiz and Ojibway[9–16]; site 2, west Hudson Strait cores HU85027-068[21], 90023-085[14], -099[14], -101[15]; site 3, east Hudson Strait cores HU85027-057[21], 90023-045[15], -064[14], 93034-004[17]; site 4, Cartwright saddle[19] cores HU87033-017, -018; and site 5, Orphan knoll[20] cores HU91045-094 and MD95-2024.

Before its demise, the Hudson Bay ice mass and the associated proglacial lakes contained a combined volume[11] estimated at 5×10^{14} m^3; however, >50% of this was ice that could not have left the Hudson Strait as rapidly as water from the lakes. So to calculate the peak freshwater flux to the Labrador Sea, we consider only the water in lakes Agassiz and Ojibway. The approximate volume of Lake Ojibway[9,11] before its abrupt northward drainage was 10^{14} m^3. The volume of Lake Agassiz at that time is not well constrained, but we follow Veillette[11] in assuming that the volume approximately equalled that of Ojibway. Thus the total freshwater volume released by drainage of both lakes is $\sim 2 \times 10^{14}$ m^3. Before drainage, the lake surfaces stood $\geqslant$175 m above the contemporaneous sea level[9,11], providing a large initial hydraulic head that drove the outburst once a conduit to the sea opened.

The stratigraphy of the Hudson and James Bay lowlands[9,11,16] (Fig. 1) ubiquitously records the abrupt lake drainage: glacial-marine sediments lie directly above the proglacial lake sediments. Additional evidence for the lake outburst is the 5–80-cm-thick, red-coloured, haematite-rich sediment layer traceable for 700 km in cores from the western to the eastern reaches of the Hudson Strait[14,15] (Fig. 1). Regional stratigraphic correlations and provenance studies[15] suggest that the Hudson Strait 'red bed' shared a common source with red glacial deposits in north-central Hudson Bay and red-brown glaciolacustrine sediments in the former Agassiz and Ojibway basins[9–11,16]. The simultaneous deposition of the red bed throughout the Hudson Strait at a time in the glacial period when the strait was free of ice[14,17] required an extraordinary sediment transport mechanism; the catastrophic outburst flood released from lakes Agassiz and Ojibway probably provided this mechanism.

We evaluated the outburst drainage model, which would have resulted in high freshwater flux and long-range sediment dispersal, by running numerical simulations of plume deposition in the Hudson Strait. The discharge resulting from instantaneous removal of the ice dam was estimated, and we then used an oceanic plume sedimentation model[18] to predict the distribution of sediment

Table 1 Dates on drainage of lakes Agassiz and Ojibway

Sample site	Interval (cm)	Laboratory no.	Ref.*	Lat., lon.† (°N, °W)	Radiocarbon age‡ (^{14}C yr BP ± 1σ)	ΔR§ (yr)	Cal. age‖ (cal. yr BP)	1σ range¶ (cal. yr BP)
SE Hudson Bay								
Post-dates drainage; dates marine incursion								
SE James Bay		Qu 122	9	53.35, 77.57	8,280 ± 160			
SE James Bay		Qu 124	9	53.35, 77.57	8,150 ± 180			
SW James Bay		GSC 897	16	50.22, 84.30	8,160 ± 160#			
SW James Bay		GSC 880	16	51.93, 84.53	8,120 ± 140#			
					(8,150 ± 50)☆	310	8,280	8,330–8,160
West Hudson Strait								
Post-dates drainage; above red bed								
90023-085	98–100	TO 3265	14	62.62, 76.38	8,170 ± 140	130	8,420	8,600–8,320
Pre-dates drainage; below red bed								
90023-101	365–367	AA 12888	15	63.05, 74.30	8,260 ± 60			
90023-099	320–325	AA 12887	14	63.07, 74.57	8,270 ± 70			
85027-068	989–996	TO 751	21	63.08, 74.31	8,310 ± 70			
					(8,280 ± 40)	130	8,550	8,650–8,490
East Hudson Strait								
Post-dates drainage; above red bed								
93034-004	19–21	CAMS 25762	17	61.22, 66.43	8,030 ± 60			
90023-045	480–483	AA 17380	15	60.95, 66.14	8,155 ± 130			
90023-064	460–462	TO 3263	14	61.13, 70.58	8,160 ± 150			
					(8,065 ± 50)	85	8,380	8,440–8,325
Pre-dates drainage; below red bed								
85027-057	814–822	TO 749	21	61.07, 66.43	8,140 ± 70			
93034-004	78–80	AA 13055	17	61.22, 66.43	8,395 ± 70			
90023-045	777–779	AA 11879	15	60.95, 66.14	8,490 ± 200			
					(9,280 ± 50)	85	8,610	8,740–8,520

* References cited provide additional sample information.
† Positions in decimal degrees; also see Fig. 1.
‡ Radiocarbon dates given as conventional, δ^{13}C-normalized ^{14}C ages (no reservoir correction).
§ See Table 2, Fig. 1 and text for derivation of local ΔR values.
‖ Calibrated date (cal. yr) converted[26] from weighted mean ^{14}C age using local ΔR values. Mean calibrated age between bounding dates on lake drainage is 8,470 cal. yr BP.
¶ Note that calibrated age ranges are asymmetrical due to the nonlinear ^{14}C calibration curve.
# In accord with laboratory protocol, GSC dates are reported here with 2σ errors; corresponding 1σ errors were used when calculating weighted means from these dates.
☆ Parentheses enclose weighted averages of preceding ^{14}C dates.

Table 2 ^{14}C ages of live-collected Hudson Bay shells

Laboratory no.	Collection site (lat. °N, lon. °W)*	Collection year (AD)	Radiocarbon age (years ± 1σ)†	Model age (years)‡	ΔR (years)§
East Hudson Strait and Ungava Bay					
CAMS-33148	60.41, 64.83	1948	630 ± 50	480	150
CAMS-34644	59.22, 65.75	1947	540 ± 50	480	60
CAMS-34654	59.48, 65.25	1950	650 ± 50	480	170
CAMS-46546	61.63, 71.97	1920	500 ± 50	460	40
CAMS-46550	60.83, 69.93	1950	620 ± 40	480	140
CAMS-46555	60.07, 69.43	1949	430 ± 40	480	–50
GSC-6107	59.22, 65.75	1947	480 ± 40	480	0
TO-5980	59.22, 65.75	1947	650 ± 40	480	170
	n = 8	Mean:	560		85
West Hudson Strait and North Hudson Bay					
CAMS-33144	64.40, 77.93	1953	760 ± 50	480	280
CAMS-33146	66.47, 86.20	1955	690 ± 50	480	210
CAMS-33149	63.00, 82.65	1954	690 ± 50	480	210
CAMS-34647	63.60, 82.00	1953	480 ± 50	480	0
CAMS-34648	64.33, 75.58	1954	600 ± 50	480	120
CAMS-46547	62.95, 81.84	1954	510 ± 40	480	30
CAMS-46549	63.00, 82.65	1954	590 ± 40	480	110
CAMS-46551	64.23, 76.55	1954	430 ± 40	480	–50
CAMS-46552	63.68, 80.20	1953	560 ± 40	480	80
CAMS-46556	64.23, 76.55	1954	590 ± 40	480	110
CAMS-46557	63.00, 82.65	1954	530 ± 50	480	50
CAMS-46559	64.23, 76.55	1954	520 ± 50	480	40
CAMS-46560	63.60, 82.00	1953	670 ± 50	480	190
CAMS-47241	66.92, 81.33	1955	810 ± 40	480	330
CAMS-47244	62.98, 82.69	1954	610 ± 40	480	130
TO-5977	64.40, 77.93	1953	690 ± 50	480	210
	n = 16	Mean:	610		130
SE Hudson Bay and James Bay					
CAMS-46545	56.50, 77.00	1920	630 ± 40	460	170
CAMS-46561	56.25, 76.33	1920	580 ± 50	460	120
CAMS-46755	52.00, 79.50	1941	970 ± 40	475	495
CAMS-46757	52.95, 79.00	1920	720 ± 40	460	260
CAMS-46759	52.00, 79.50	1920	1,050 ± 40	460	590
CAMS-46760	52.95, 79.00	1920	740 ± 40	460	280
CAMS-46761	52.60, 78.75	1920	810 ± 40	460	350
CAMS-47247	55.28, 77.75	1949	560 ± 50	480	80
CAMS-48978	53.12, 79.86	1920	740 ± 40	460	280
CAMS-48979	52.00, 79.50	1920	940 ± 40	460	480
	n = 10	Mean:	775		210

* Live shell sample locations in decimal degrees.
† Laboratory-reported, conventional, δ^{13}C-normalized ^{14}C ages.
‡ Model-derived mean surface ocean ages for the year of collection[22].
§ ΔR = measured shell radiocarbon age minus modelled surface ocean age. Regional means of the ΔR values are used in calibration[26] of ages for the lake outburst event (Table 1).

resulting from an event of this magnitude. The simulation predicted deposit thicknesses of ~50 cm in the western Hudson Strait, thinning to ~30 cm in the eastern Hudson Strait. The approximate agreement of modelled deposit thicknesses with the observed red bed[14,15,17] supports the interpretation that final drainage of lakes Agassiz and Ojibway produced a massive freshwater pulse to the Labrador Sea (Fig. 1).

Evidence for a freshwater pulse is also found beyond the Hudson Strait. Cores from Cartwright saddle on the Labrador shelf (Fig. 1) exhibit a 0.6‰ reduction in the δ^{18}O of planktonic foraminifera between 8.5 and 8.3 cal. kyr ago (~7.8–7.6 ^{14}C kyr)[19]. Farther southeast, piston cores from the flank of Orphan knoll (Fig. 1) show increased offsets between the δ^{18}O compositions of planktonic foraminifera *Globigerina bulloides* and left-coiling *Neogloboquadrina pachyderma* (shallow- and deep-dwelling species, respectively)[20]. The offset increases from 0.8‰ before the freshwater pulse to 1.3‰ during the pulse, due to a 0.5‰ reduction in the *G. bulloides* values. This isotopic shift is comparable to that at Cartwright saddle and indicates lower sea surface salinities and increased water-mass stratification throughout the western Labrador Sea[20]. Thus data from various sites support a large freshwater plume entering the Labrador Sea in the early Holocene. We determined the calendar age of the Laurentide lake outburst to ascertain whether this freshwater input coincided with onset of the '8.2-kyr' cold event.

The published radiocarbon dates constraining the final Agassiz–Ojibway drainage are on marine carbonates from the Hudson and James Bay lowlands[9,12,16] and the Hudson Strait[14,15,17,21] (Table 1; Fig. 1). Because of the pattern of ice marginal recession along the southern margin of Hudson Bay, the post-glacial sea reached its highstand throughout that region simultaneously. Dates on fossil marine bivalves from uplifted basal post-glacial marine sediments in the Hudson Bay lowlands constrain the time of initial marine incursion, and thus also provide limiting ages that post-date drainage of lakes Agassiz and Ojibway (Table 1; Fig. 1)[9,16]. In the Hudson Strait (Fig. 1), the radiocarbon ages bounding the freshwater pulse are on bivalves and foraminifera collected above and below the red bed in marine sediment cores (Table 1; Fig. 1). In earlier work on the overall chronostratigraphy of the Hudson Strait[14,15,17,21], many more dates were obtained than we include in Table 1. We excluded many dates because sediment reworking obfuscated their stratigraphic context. Of the remaining dates, we consider only those that most closely constrain deposition of the red bed.

Conversion of ^{14}C dates to the calendar-year timescale allows comparison with events in ice-core chronologies[2,6] produced by counting of annual layers, but precise calibration cannot be performed without a correction for the local marine ^{14}C reservoir effect[22]. The local reservoir correction is the sum, in radiocarbon years, of the mean global surface ocean reservoir age (R) plus any local deviation (ΔR) from the contemporaneous global-mean ocean age[22]. Detailed comparisons between radiocarbon dates from different regions or reservoirs (for example, the atmosphere) require an estimate of ΔR. In the past, ΔR values were not well established; so in earlier work, reservoir corrections of 400–450 years (that is, ΔR = 0) were applied to shallow marine dates. Here we estimate local ΔR values using radiocarbon dates on 34 museum shell

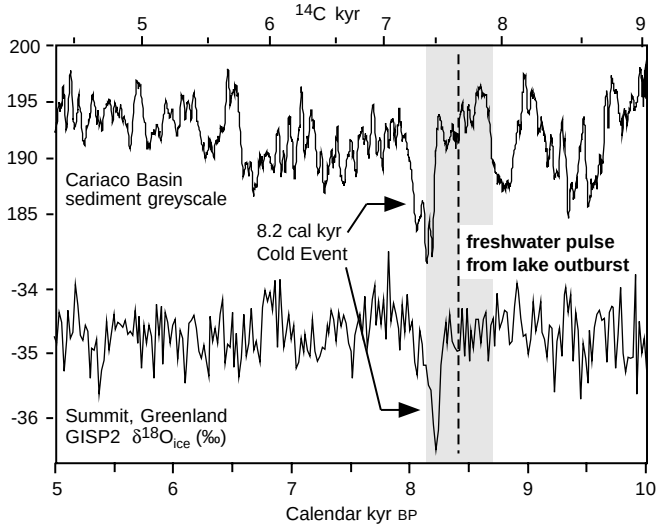

Figure 2 Climate proxy records of the '8.2-kyr' cold event. Both ^{14}C (top) and calendar (lower) timescales are given. Upper curve shows Cariaco basin greyscale record; reduced greyscale values indicate increased zonal wind speed due to high-latitude cooling[5]. Timescale of greyscale variations differs from that in ref. 5 due to subsequent work by those authors; data on the revised timescale are available from the World Data Center-A for Paleoclimatology (http://www.ngdc.noaa.gov/paleo). Lower curve shows bidecadal $\delta^{18}O$ values of ice from the GISP2 ice core[6], interpreted to reflect primarily the temperature of precipitation over Summit, Greenland; more negative values indicate colder temperatures. Also shown is age for the lake drainage event: 8,470 cal. yr BP or ~7.7 ^{14}C kyr (vertical dashed line); extremes of the 1σ cal. age ranges on the bounding dates (Table 1) give an error range of 8,160–8,740 cal. yr BP (shaded).

specimens that were collected alive in the Hudson Bay region from AD 1920 to 1955, before significant contamination of the atmosphere with bomb radiocarbon (Table 2). The ages of these shells range from 430 to 1,050 ^{14}C yr (1σ errors range from 40 to 50 yr). Despite the observed variability, the ages typically exceed 550 yr and the means of ages from each region increase consistently with distance from the open Labrador Sea (Fig. 1). By comparing the shell dates with modelled mean-ocean reservoir age data[22], we derive ΔR values for the southeastern Hudson Bay and James Bay of 310 ± 50 yr, for the northern Hudson Bay and western Hudson Strait of 130 ± 50 yr, and for the eastern Hudson Strait of 85 ± 50 yr (Table 2; Fig. 1).

We identify two possible causes of the higher ΔR values (that is, lower initial ^{14}C activities) for the marine carbon pools in the Hudson Bay and Hudson Strait: (1) runoff draining Palaeozoic limestone bedrock and carbonate-rich glacial sediments in the region provides dissolved ^{14}C-free bicarbonate[23]; (2) persistent sea-ice coverage inhibits air–sea ^{14}C equilibration. Modelling[24] suggests that the 7–8 months of seasonal sea ice in the Hudson Strait[25] could cause an apparent ageing of the marine ^{14}C reservoir by 150–200 yr, slightly more than observed (Table 2; Fig. 1). However, despite a shorter sea-ice season, James Bay shells have the highest ΔR values in the region (Table 2; Fig. 1). Significant runoff from carbonate-rich areas enters James Bay, thus both sea ice and inputs of ancient carbon seem to contribute to the observed pattern in ΔR values. To calibrate ^{14}C dates from the deglacial period 8.8–7.5 cal. kyr ago , we must evaluate possible differences in the factors influencing ΔR. During the time of interest, high inputs of melt water from the residual ice sheet[12] (Fig. 1) probably lengthened the sea-ice season[25]. Additionally, ^{14}C-free bicarbonate input was probably higher due to the abundance of fresh, glacially abraded Palaeozoic carbonate[23]. The effects on ΔR of differing water masses and current patterns during deglaciation are not known, although the lower percentage of Labrador Sea surface water (pre-bomb ΔR = 0) in the mixed Hudson Bay water mass[25] may have produced larger ΔR values during deglaciation. Taken together, these effects imply that the regional ΔR values in Table 2 are conservative (that is, low) with respect to those ~8,000 years ago.

The ΔR values derived here facilitate conversion of radiocarbon ages for the final Agassiz–Ojibway drainage into calendar ages using the marine calibration scheme in CALIB 3.03A[26]. We calculated the age of the freshwater pulse (8,470 cal. yr before present, BP) as the midpoint between means of both the younger and older event-bounding calibrated ages (Table 1). Within the limits of annual ice-core layer counting, radiocarbon dating, ΔR estimates, and ^{14}C-to-calendar year conversion, the age derived here for final northward drainage of lakes Agassiz and Ojibway coincides with the 8,400 ± 100 cal. yr BP onset of climate cooling in Greenland and elsewhere[2–8] (Fig. 2).

The cataclysmic release of 2 ×10^{14} m^3 of lake water over 1, 10 or 100 years would have increased the freshwater flux to the Labrador Sea by 6, 0.6 or 0.06 Sv (1 Sv = 10^6 m^3 s^{-1}), respectively. Numerical simulation of the Hudson Strait redbed deposit suggests that drainage occurred in less than one year, but the available chronology does not yield a precise duration. Results from ocean circulation models[27–29] suggest that excess freshwater discharges of 0.06–0.12 Sv can reduce the formation rates of Labrador Sea Intermediate Water (LSW) and North Atlantic Deep Water (NADW), thereby strongly affecting ocean heat transport. These simulations do not specifically apply to the lake outburst case, however, because the excess discharges were prescribed for periods of >500 years in the models[27–29]. Although the ocean freshening due to Agassiz–Ojibway drainage was of shorter duration, the lakewater pulse was preceded by an interval (600–900 years) of somewhat reduced sea surface salinity in the Labrador Sea. This previous low-salinity interval, recorded by reduced $\delta^{18}O$ values and increased ice-rafted detritus at both Cartwright saddle[19] and Orphan knoll[20] (Fig. 1), apparently resulted from the advance and subsequent breakup of a partly marine-based northern Labrador ice sheet[17].

The low sea surface salinities resulting from the Agassiz–Ojibway outburst propagated southeast from Hudson Strait, producing more pronounced freshening in the region of LSW formation (Fig. 1) than at the more distant NADW formation sites[7]. The present northward ocean heat transport associated with formation of LSW is 0.3 PW (1 PW = 10^{15} W), half that due to formation of NADW (0.6 PW)[30]. If the formation of both LSW and NADW ceased during the Younger Dryas cold event, but only LSW formation was disrupted during the '8.2-kyr' event, then for the latter event we might expect regional atmospheric cooling of one-third the magnitude as that during the Younger Dryas. This scenario

undoubtedly oversimplifies ocean circulation and climate boundary conditions, but the resulting prediction of the relative amplitudes of the two cold events approximates the relative cooling observed in proxy records that contain both events[2–6].

Evidence presented here—of a large freshwater pulse from the final outburst drainage of lakes Agassiz and Ojibway, together with the revised timing of this pulse (~8,470 cal. yr BP, or ~7.7 ^{14}C kyr BP)—directly supports the hypothesis[3,7,8] that an increase in freshwater flux modified ocean circulation, thereby causing the observed '8.2-kyr' climate cooling. This result provides perspective both on the sensitivity of ocean circulation to freshwater inputs and on the climate oscillations of the present interglacial period. Specifically, our findings suggest that in the case of the '8.2-kyr' event, the thermohaline circulation responded to exceptionally strong forcing: initiation of the most abrupt and widespread climate shift known from the past 10,000 (calendar) years required a massive, albeit short-lived, perturbation of the North Atlantic freshwater balance. □

Received 26 March; accepted 8 June 1999.

1. Broecker, W. S. Thermohaline circulation, the Achilles heel of our climate system: Will man-made CO_2 upset the current balance? *Science* **278,** 1582–1588 (1997).
2. Alley, R. B. *et al.* Holocene climatic instability: a prominent, widespread event 8200 yr ago. *Geology* **25,** 483–486 (1997).
3. Street-Perrott, F. A. & Perrott, R. A. Abrupt climate fluctuations in the tropics: the influence of the Atlantic Ocean circulation. *Nature* **343,** 607–612 (1990).
4. Bond, G. *et al.* A pervasive millennial-scale cycle in North Atlantic Holocene and Glacial climates. *Science* **278,** 1257–1266 (1997).
5. Hughen, K. A., Overpeck, J. T., Trumbore, S. & Peterson, L. C. Rapid climate changes in the tropical Atlantic region during the last deglaciation. *Nature* **380,** 51–54 (1996).
6. Stuiver, M., Grootes, P. M. & Braziunas, T. F. The GISP2 ^{18}O record of the past 16,500 yrs and the role of the sun, ocean and volcanoes. *Quat. Res.* **44,** 341–354 (1995).
7. Klitgaard-Kristensen, D., Sejrup, H. -P., Haflidason, H., Johnsen, S. & Spurk, M. A regional 8200 cal. yr BP cooling event in northwest Europe, induced by final stages of the Laurentide ice-sheet deglaciation? *J. Quat. Sci.* **13,** 165–169 (1998).
8. von Grafenstein, U., Erlenkeuser, H., Müller, J., Jouzel, J. & Johnsen, S. The cold event 8200 years ago documented in oxygen isotope records of precipitation in Europe and Greenland. *Clim. Dyn.* **14,** 73–81 (1998).
9. Hardy, L. La déglaciation et les épisodes lacustre et marin sur les versants de la partie québécoise des basses terres de la baie de James. *Geogr. Phys. Quat.* **31,** 261–273 (1977).
10. Teller, J. T. in *The Geology of North America* Vol. K-3, *North America and Adjacent Oceans during the Last Deglaciation* (eds Ruddiman, W. F. & Wright, H. E. Jr) 39–69 (Geol. Soc. of America, Boulder, Colorado, 1987).
11. Veillette, J. J. Evolution and paleohydrology of Glacial Lakes Barlow and Ojibway. *Quat. Sci. Rev.* **13,** 945–971 (1994).
12. Dyke, A. S. & Prest, V. K. Paleogeography of northern North America, 18000–5000 years ago. (Map 1703A, Scale 1:12500000, Geol. Surv. of Canada, Ottawa, 1989).
13. Andrews, J. T. & Falconer, G. Late glacial and postglacial history and emergence of the Ottawa Islands, Hudson Bay, N.W.T. : Evidence on the deglaciation of Hudson Bay. *Can. J. Earth Sci.* **6,** 1263–1276 (1969).
14. Andrews, J. T. *et al.* Final stages in the collapse of the Laurentide Ice Sheet, Hudson Strait, Canada, NWT: Based on ^{14}C AMS dates and magnetic susceptibility logs. *Quat. Sci. Rev.* **14,** 983–1004 (1995).
15. Kerwin, M. W. A regional stratigraphic isochron (ca. 8000 ^{14}C yr B. P.) from the final deglaciation of Hudson Strait. *Quat. Res.* **46,** 89–98 (1996).
16. Skinner, R. G. Quaternary stratigraphy of the Moose River basin, Ontario. *Geol. Surv. Can. Bull.* **225** (1973).
17. Jennings, A. E., Manley, W. F., MacLean, B. & Andrews, J. T. Marine evidence for the last glacial advance across eastern Hudson Strait, eastern Canadian Arctic. *J. Quat. Sci.* **13,** 501–514 (1998).
18. Syvitski, J. P., Skene, K. I., Nicholson, M. K. & Morehead, M. D. Plume 1. 1: Deposition of sediment from a fluvial plume. *Comput. Geosci.* **24,** 159–171 (1998).
19. Andrews, J. T., Keigwin, L., Hall, F. R. & Jennings, A. E. Late Quaternary (12 ka) sediment and meltwater events on the Labrador shelf: Evidence from high-resolution cores in Cartwright Saddle (54–55°N). *J. Quat. Sci.* (in the press).
20. Bilodeau, G., Hillaire-Marcel, C., de Vernal, A. & Stoner, J. Changes in vertical structure of Labrador Sea water masses during the last 25 ka based on oxygen isotopes in planktic and benthic foraminifera. *Geosci. Can.* **23,** (Suppl: Quebec 1998 Abstr.) 18–19 (1998).
21. Vilks, G., MacLean, B., Deonarine, B., Currie, C. G. & Moran, K. Late Quaternary paleoceanography and sedimentary environments in Hudson Strait. *Geogr. Phys. Quat.* **43,** 161–178 (1989).
22. Stuiver, M. & Braziunas, T. F. Modeling atmospheric ^{14}C influences and ^{14}C ages of marine samples to 10,000 BC. *Radiocarbon* **35,** 137–189 (1993).
23. Karrow, P. F. Carbonates, granulometry, and color of tills on the south-central Canadian Shield and their implications for stratigraphy and radiocarbon dating. *Boreas* **21,** 379–391 (1992).
24. Bard, E. *et al.* The North Atlantic atmosphere-sea surface ^{14}C gradient during the Younger Dryas climatic event. *Earth Planet. Sci. Lett.* **126,** 275–287 (1994).
25. Drinkwater, K. F. in *Canadian Inland Seas* (ed. Martini, I. P.) 237–264 (Elsevier, New York, 1986).
26. Stuiver, M. & Reimer, P. J. Radiocarbon calibration program Rev 3.0.3A - Mac Test Version #6. *Radiocarbon* **35,** 215–230 (1993).
27. Rahmstorf, S. On the freshwater forcing and transport of the Atlantic thermohaline circulation. *Clim. Dyn.* **12,** 799–811 (1996).
28. Fanning, A. F. & Weaver, A. J. Temporal-geographical meltwater influences on the North Atlantic Conveyor: Implication for the Younger Dryas. *Paleoceanography* **12,** 307–320 (1997).
29. Manabe, S. & Stouffer, R. J. Coupled ocean-atmosphere model response to freshwater input: Comparison to Younger Dryas event. *Paleoceanography* **12,** 321–336 (1997).
30. Talley, L. D. in *Mechanisms of Millennial-scale Global Climate Change.* (eds Clark, P. U., Webb, R. & Keigwin, L.) (AGU Monogr., Am Geophys. Union, Washington DC, in the press).

Acknowledgements. We thank the Canadian Museum of Nature for providing archived live-collected shells, and G. Bond, D. Fisher, B. MacLean and J. Teller for comments on the manuscript. This work was supported by the Terrain Sciences Division, Geological Survey of Canada, and the US NSF (A.E.J. and J.T.A.).

Correspondence and requests for materials should be addressed to D.B. (e-mail: barberdc@ucsub.colorado.edu)

Asynchronous deposition of ice-rafted layers in the Nordic seas and North Atlantic Ocean

J. A. Dowdeswell*, A. Elverhøi†, J. T. Andrews‡ & D. Hebbeln§

** Bristol Glaciology Centre, School of Geographical Sciences, University of Bristol, Bristol BS8 1SS, UK*
† Department of Geology, University of Oslo, Postboks 1047, Blindern, N-0316 Oslo, Norway
‡ Institute of Arctic and Alpine Research and Department of Geological Sciences, University of Colorado, Boulder, Colorado 80309, USA
§ FB Geowissenschaften, University of Bremen, Postfach 330440, D-28344 Bremen, Germany

Instabilities in ice-stream flow within the North American Laurentide Ice Sheet, leading to the periodic release of armadas of icebergs into the North Atlantic Ocean over the past 60,000 years, have produced extensive layers of coarse-grained iceberg-rafted debris (Heinrich layers) in North Atlantic sediments[1,2]. Correlation of these layers with iceberg-discharge events from the ice sheets on Greenland, Iceland and Scandinavia, suggested in previous studies for some Heinrich layers and in some areas[3–5], would imply that ice-sheet instability had been synchronous across the North Atlantic, presumably in response to a common environmental cause. Here we show a lack of widespread systematic correlations, both between ice-rafted debris layers in different sediment cores from the Nordic seas, and between the Nordic layers and the North Atlantic Heinrich layers. This suggests that the full-glacial Nordic ice sheets did not exhibit unstable behaviour coincident with iceberg discharge from the vast Hudson Bay drainage basin of the Laurentide Ice Sheet[6,7]. Off the Hudson Strait, significant ice-sheet discharge of melt water is indicated by size-sorted sandy and muddy turbidite sediments, different from the poorly sorted debris flows which dominate sedimentation on the margins of the Nordic seas[8–10]. Together, these results suggest that the dynamics of Quaternary ice sheets surrounding the Nordic seas were different from the outlet glacier draining the Hudson Bay basin, and they provide evidence against a common circum-North-Atlantic mechanism driving the discharge of icebergs.

A number of marine geological studies have demonstrated that huge numbers of icebergs, derived mainly from the Hudson Strait, produced a series of six rapidly deposited[11] Heinrich layers of iceberg-rafted debris (IRD). These distinctive layers range from about one metre to a few centimetres in thickness, and can be traced for more than 3,000 km across the North Atlantic[1,2]. However, although many sediment cores have been examined from the Nordic seas (Fig. 1), coarse-grained layers of the thickness and spatial continuity of the Heinrich layers have not been identified. Correlative IRD events have so far been found only in some areas and for some of the Heinrich events[3–5,12,13] (Fig. 2).

Cores from sites adjacent to outlet glaciers of the Fennoscandian, Svalbard-Barents Sea and Greenland ice sheets (Fig. 1b) show that there is little evidence for a systematic regional correlation of IRD layers across the Nordic seas, nor is there a consistent linkage with the North Atlantic Heinrich layers (Fig. 2). A detailed study of IRD